



Optimization of Thermal Decomposition Conditions of Bone to Achieve the Highest Percentage of Crystalline Phase in Bone Char using Gene Expression Programming and Artificial Neural Network

F. Fatahi, G. R. Khayati*

Department of Materials Science and Engineering, Shahid Bahonar University of Kerman, Kerman, Iran

P A P E R I N F O

Paper history:

Received 04 August 2020

Received in revised form 20 October 2020

Accepted 29 October 2020

Keywords:

Artificial Neural Networks

Bone Char

Gene Expression Programming

Modeling

Pyrolysis Conditions

A B S T R A C T

Bone char (BC) is one of the most common adsorbent with extensive applications in the removal of pollutions. The adsorption capability of BC is proportional to the crystalline index, i.e., the atomic ratio of Ca/P. This study is an attempt to model the crystalline index of BC that by thermal decomposition of natural bone using artificial neural network (ANN) and genetic expression programming (GEP). In this regard, 100 various experimental data used to construct the ANN and GEP models, separately. Through the data collection step, heating rate, the type of precursor, calcination temperature, and residence time selected as the inputs for the preset output as Ca/P ratio. The results reveal that the minimum amount of Ca/P ratio are at the heating rate 10 °C/min, HNO₃ 1.6 M as activation agent, calcination temperature 1000 °C, and residence time 2 h. R squared indices is used to compare the performance of extracted models. Finally, the best ANN uses to investigate the effect of each practical variable by sensitivity analysis and revealed that the residence time is the most effective parameter on the crystalline index while acid activation is of secondary importance.

doi: 10.5829/ije.2021.34.01a.21

1. INTRODUCTION

Due to the increasing growth of various industries and industrial products around the world, challenges about the severe damages to the environment are increasing. Therefore, to reduce the environmental degradations, it is necessary to reduce the amount of waste by consideration of a logical and cost-effective solution. Solid waste, e.g., animal waste, are a potential source of renewable materials. Thermal conversion of solid waste into char has been widely studied as a promising solution for waste disposal. During this conversion, a valuable by-product is produced that can be used in many fields of industrial production to reduce the environmental damages [1, 2]. Bone char (BC) is a black, porous, granular substance that prepared by heating of animal bones. It is one of the most common sorbents with unique characteristics including eco-friendly, accessible, cheap, and excellent

regenerating specification. Adsorption of pollution is one of the most common applications of BC, e.g., water treatment process, in the industry. It traditionally uses as discoloration agent in the sugar industry [3, 4]. Adsorption of F, Cd, Zn, Ni, Cu and As from aqueous solution with low cost are the other applications of BC. Therefore, finding a solution to produce and control the characteristics of BC is of great importance [5, 6]. There is a significant dependency between the compositions of BC to its preparation methods. There are 50-80 wt.% hydroxyapatite, 10-16 wt.% CaCO₃, and 7-10 wt.% carbon in the chemical composition of BC. Incomplete combustion of natural bones with controlled oxygen is the main approach for the preparation of BC. Table 1 illustrates the physical and chemical properties and application of BC that have been prepared by different methods. There is a strong dependency between the crystallinity index of BC (i.e., the ratio of Ca/P) on its

*Corresponding Author Institutional Email: khayati@uk.ac.ir (G. R. Khayati)

capacity as an adsorbent agent [7]. In this regard, optimization of the amount of Ca/P ratio plays a key role for design and preparation of BC with a better adsorption performance. P and Ca are the main constituents of bone. The other constituents with lower contents are Na, C, Mg, and O. In general, stoichiometric amount of Ca/P ratio in bone is 1.67 [8, 9]. However, based on Table 1, the Ca/P ratio is completely variable and the charring of animal bones is the main preparation method of BC. Some advantages including low production and activation process caused the evolution of charring of animal bones as a promising approach for the preparation of BC. Unfortunately, this process suffers from the comprehensive investigation on the analysis of complicated interaction between the practical variables including pre-process or activation of bones by acidic solutions, calcination temperature, heating rate, and residence time. To the best of our knowledge, several methods have been used to produce BC. However, no research has been done to model the crystalline index of BC based on practical variables, so far. Hence, illustration of reliable models based on experimental data is strongly proposed to enhance the performance of BC. This study aims at constructing new predictive models based on gen expression programming (GEP) and artificial neural network (ANN), for determination of the Ca/P ratio as a function of practical variables. To construct these models, 100 reliable trails were done for the preparation of BC. The data are used to train and test GEP and ANN models. The calcination temperature changed between 400 °C to 1000 °C, the residence time is considered in the range of 1 to 4 h, and the heating rate changed from 5 to 12 °C/min. The performance of both models are compared to each other. Finally, the effect of

each practical variable is investigated by sensitivity analysis.

2. MATERIALS AND METHODS

The thigh bone of cow is used as a precursor to prepare the bone char. As a first step, selected thigh bone washed for 2 h in boiling deionized water to wipe out meat and fat residues and left 24 h to dry. Then, the dried bones are crashed (with the particle size lower than 1 mm) and uses as mother sample for the preparation of BC.

2. 1. Specimen Preparation

A CVD furnace equipped with the ceramic holder is used through the calcination step. At first, the origin bones sample divide into 100 parts. 60 parts directly heated to prepare BC. The remained 40 parts pre-processed by the addition of 490 mL of HNO₃ (with various concentrations including 0.49, 1.1, 1.6 M) to 50 gr of crashed bones in Erlenmeyer flask on a hot plate at the temperature of 80 °C. The prepared solution is mixed for 24 h. Then, the solution is cleared, and the pre-processed samples locate in a porcelain capsule. Finally, the prepared BC sample stored in a micro tubes for further analysis. As shown in Table 2, the BC samples that directly used identified by 1 and the pre-processed bones with 0.49, 1.1, and 1.6 M HNO₃ solutions are identified by 2, 3, and 4, respectively. BC samples synthesized under the special conditions of pyrolysis including the calcination temperature (400-1000 °C), heating rate (5-12 °C/min), residence time (1-4 h) and argon gas (400 mL/min). EDX analysis is utilized to investigate the weight percentages of Ca and P elements to calculate the crystalline index (Table 2).

TABLE 1. Chemical composition of BC as a function of preparation condition and its applications

Ref.	Total Ca (wt.%)	Total P (wt.%)	Total C (wt.%)	Hydroxyapatite (%)	Application of BC
[10]	-	-	9-11	70-76	Adsorption of toxic ions
[11]	-	-	11.0	76	Adsorption of fluoride
[12]	-	13.4	12.5	-	Filtrations of P
[13]	28	15.2	13	-	Filtrations of P
[14]	-	15	6.3	85	Adsorption of fluoride
[15]	39	20	-	80	Water treatment
[16]	30.7	14	-	69	Filtrations of P
[17]	27.1	12.7	18.0	-	Used as P-fixing soil influenced by root-mycorrhiza-bio char interactions
[18]	18.5	14.9	11.2	-	Improvement the phosphorus-cadmium-interaction
[17]	33.7	15.3	8.2	-	Used as P-fixing soil
[19]	23.9	15.7	-	89	Adsorption of Cr (III) from water solution
[20]	24.2	11.5	3.8	-	Absorption the methylene blue
[21]	23.8	13	10.4	56	Improvement of the transformations of P in plant-based structure
[22]	-	-	10.0	80-90	Enhancement of photocatalytic performance by ZnO/BC composites

TABLE 2. Summary of the experimental design used to the synthesis of BC

No.	Inputs			Output	
	Precursor ^a	Calcination temperature (°C)	Heating rate (°C/min)	Residence time (h)	Ca/P Ratio
1	3	1000	7	1	1.31
2	4	400	5	1	1.27
3	3	700	5	4	1.45
4	3	400	12	3	1.41
5	2	1000	5	3	1.72
6	2	400	7	4	1.92
7	4	700	7	3	1.03
8	2	700	12	1	1.69
9	1	900	10	2	2.02
10	3	800	10	2	1.30
11	1	500	7	2	2.30
12	1	600	10	3	2.14
13	1	800	5	1	2.24
14	3	500	10	1	1.46
15	4	600	7	4	1.05
16	3	900	12	3	1.17
17	2	600	5	2	1.93
18	2	500	10	4	1.79
19	2	800	7	3	1.75
20	4	500	12	2	0.99
21	4	900	5	1	1.03
22	1	800	12	4	1.97
23	4	700	10	2	0.96
24	2	600	12	1	1.74
25	1	500	5	3	2.34
26	1	400	10	1	2.28
27	1	1000	12	2	1.92
28	1	900	7	4	2.07
29	4	800	10	3	0.89
30	3	400	5	2	1.63
31	2	1000	10	4	1.55
32	3	600	5	4	1.50
33	2	900	7	2	1.73
34	1	700	7	1	2.23
35	3	600	7	1	1.50
36	4	1000	7	2	0.91
37	4	900	10	1	0.88
38	2	800	12	2	1.63
39	4	500	12	4	0.95
40	1	400	12	3	2.18
41	1	700	5	4	2.22
42	2	500	5	3	1.95
43	3	700	10	3	1.33
44	2	400	10	4	1.83
45	3	800	7	4	1.35

46	3	900	12	4	1.15
47	4	600	10	3	0.99
48	3	1000	10	1	1.22
49	4	800	5	1	1.08
50	2	700	12	1	1.69
51	2	900	5	3	1.76
52	4	400	7	2	1.19
53	1	600	12	2	2.11
54	3	500	7	1	1.55
55	1	1000	7	3	2.04
56	3	700	5	2	1.49
57	1	1000	5	4	2.08
58	3	1000	12	3	1.12
59	2	500	10	2	1.83
60	3	900	5	2	1.40
61	4	500	5	3	1.18
62	2	600	7	3	1.85
63	2	800	12	1	1.65
64	4	400	12	4	1.00
65	1	900	10	1	2.04
66	3	800	10	4	1.26
67	2	400	5	1	2.04
68	2	700	10	4	1.69
69	4	600	5	4	1.11
70	4	1000	10	2	0.82
71	4	900	7	3	0.93
72	1	400	10	3	2.24
73	1	500	7	4	2.26
74	1	800	5	2	2.22
75	1	600	12	1	2.13
76	3	400	7	2	1.58
77	4	700	12	3	0.88
78	3	500	12	1	1.40
79	4	800	7	1	1.02
80	2	1000	5	1	1.76
81	2	900	12	4	1.54
82	2	700	7	2	1.82
83	3	600	10	2	1.39
84	3	800	7	3	1.37
85	1	700	12	2	2.06
86	1	700	7	1	2.23
87	4	600	12	2	0.95
88	3	1000	12	3	1.12
89	4	400	10	1	1.12
90	2	500	10	3	1.81
91	1	900	5	3	2.15
92	1	600	10	4	2.12
93	4	500	5	4	1.16

94	2	1000	7	2	1.68
95	3	400	7	4	1.53
96	1	800	5	2	2.22
97	3	700	5	3	1.47
98	3	900	12	2	1.19
99	3	600	5	1	1.56
100	4	1000	12	4	0.92

^aNumber of 1, 2, 3, and 4 refer to the sample that uses as-cleaned bone, initial bone sample modified with 0.4, 1.1, and 1.6M of HNO₃, respectively.

3. METHODOLOGY

3. 1. 1. Genetic Expression Programming (GEP)

GEP is the hybrid version of genetic algorithm (GA) and genetic programming (GP) to enhance the performance of each one [23-27]. The main elements of GEP are terminal set, fitness function, and termination condition. GEP different from GP in the way of the solution representation condition. The creation of a fixed length of character strings to show the solution as a computer model in a tree-like structure is the administered approach in GEP. These trees named expression trees (ETs) [24, 25, 28]. The operation of GEP element is performed at chromosome level and leads to the simplification in the creation of genetic diversity. Multigenics is another characteristic of GEP. Accordingly, it provides a higher capability for the solution of more complex problems. GEP elements take the value of independent input data and can convert or process them [29]. $\pm, \times, \sqrt{a, b, c}$ are typical GEP operations where a, b and c are the function sets of elements. \pm, \times and $\sqrt{\quad}$ are the terminal nodes. Karva notation or K-expression used this notation to illustrate the proposed model [23]. Besides the expression-trees, K-expression can report the proposed model in GEP. The root of ET is the first position in K-expression [27, 30]. The transformation of ET starts from the root and readsthrough the string one by one. The size of the corresponding ETs as a function of the complexity of process changes within the GEP process. As a general law, the length of each expression must be equal or less than the length of genes. Validation of the randomly selected genome is performed by the head-tail methods. Head and tail are the main components of the gene. The former composed of the function and terminal symbols, while the latter only concluding terminal symbols [28]. Selection and copy of individuals through the GEP employed the roulette wheel strategy. The validation of the population is determined by various operators, including rotation, crossover, and mutation. It is necessary to note that, rotating the sub-parts of the genome respect to the randomly chosen point was performed by rotation operators. Validation of proposed GEP models is carried out by the employment of statistical indicator, including the mean square error

(MSE; Equation (1)), correlation coefficients (Equation (2)) [31] and mean absolute percentage error (MAPE; Equation (3)).

$$MSE = \frac{1}{n} \sum_{i=1}^n (t_i - o_i)^2 \tag{1}$$

$$R^2 = 1 - \left(\frac{\sum_{i=1}^n (t_i - o_i)^2}{\sum_{i=1}^n o_i^2} \right) \tag{2}$$

$$MAPE = \frac{1}{n} \left(\sum_{i=1}^n \left| \frac{t_i - o_i}{t_i} \right| \right) \times 100 \tag{3}$$

where, o, t and n are the predicted value, the actual value and the total number of data, respectively. GEP model has higher accuracy, when MSE and MAPE are closer to zero, and R² closer to 1. Figure 1 shows the flowchart in GEP and, Figure 2 illustrates the chromosome with two genes and its decoding in GEP.

3. 1. 2. Evaluation of the Existing Models

Table 2 shows the collected experimental dataset including 100 samples. 70 samples are used in training step and 30 in testing step through the construction of GEP models. The practical parameters include the type of precursor (activated or non-activated by HNO₃), calcination temperature (°C), residence time (h), and

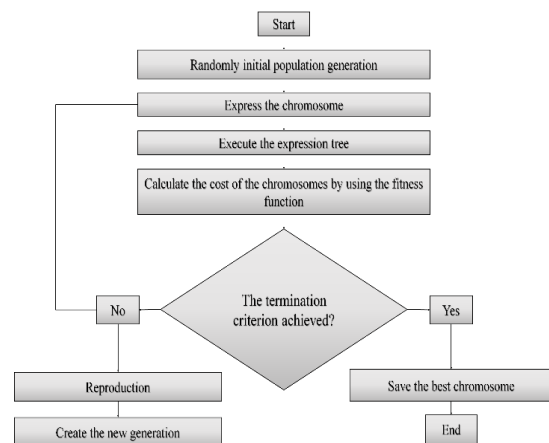


Figure 1. Flowchart of GEP

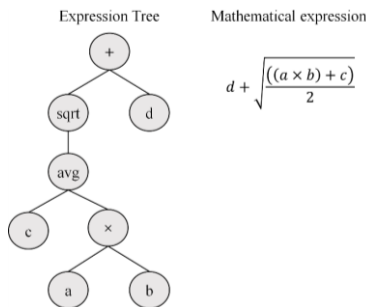


Figure 2. Representation of the typical chromosome with two genes and its decoding in GEP

heating rate (°C/min) selected as inputs. Ca/P ratio (crystalline index) is considered as the output. For GEP-based formulas, fitness (f_i), from a single program, is measured by Equation (4):

$$f_i = \sum_{i=1}^q (M - |C_{ij} - T_i|) \quad (4)$$

where, C_{ij} is the value returned by the individual chromosome, T_j the target value for the fitness case j , and (i) for fitness case and M the range of selection j . The benefit of this fitness functions is that the system can discover the optimal solution. In other words, to construct the chromosomes, fundamental functions (e.g., \ln , $3Rt$, x^2) and basic arithmetic operators (e.g., $-$, $*$, $/$, $+$) are chosen. Parameters of the training of GEP models are shown in Table 3.

3.1.3. GEP Model Results GEP proposes a distinct mathematical model for the prediction of target value. Figure 3 showed the expression-trees of the most appropriate GEP model in which d_0 , d_1 , d_2 and d_3 in the

TABLE 3. Illustration of parameters applied in GEP models

Parameters	Setting
Function set	$+$, $-$, $*$, $/$, \ln , x^2 , $3Rt$, $Atan$, $Tanh$, $Avg2$, Inv , NOT
Chromosomes	25
Head size	6
Number of genes	5
Linking function	Addition
Fitness function error type	RRSE
Mutation rate	0.002
Inversion rate	0.004
One-point recombination rate	0

order represented the type of precursor, calcination temperature, heating rate and residence time. Equation (5) gives the prediction of the Ca/P ratio obtained from GEP expression tree. In Equation (5), T_p , C_t , H_r , R_t represent the type of precursor, calcination temperature, heating rate and residence time, respectively.

$$y = A \tan \left[\tanh(T_p) - A \tan(2C_t) + \frac{41.31 - (T_p)}{R_t} \right] + \left[\tanh \left(\frac{(T_p)^2}{19.48} \right) + A \tan \left(\frac{(H_r) \times (T_p)^2}{2} \right) \right] + \tanh \left[\frac{12.86}{H_r} + \frac{1}{A \tan(T_p)} + 0.3(T_p) \right] + 24.69 \quad (5)$$

The comparison of empirical and predicted values by GEP models for Ca/P in training phase is depicted as regression plots in Figure 4.

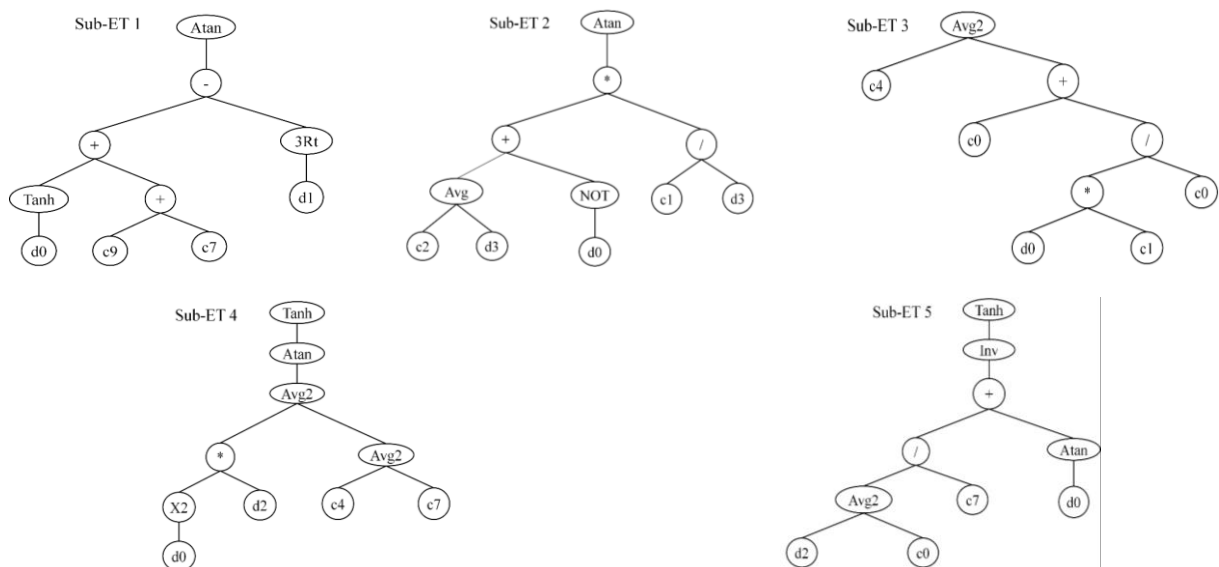


Figure 3. Expression-trees of most appropriate GEP model (d_0 : the type of precursor, d_1 : calcination temperature, d_2 : heating rate and d_3 : residence time)

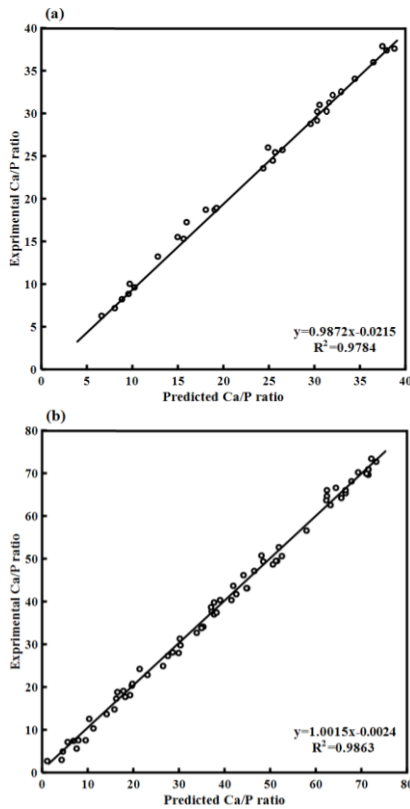


Figure 4. Illustration of (a) testing and (b) training regression in GEP model

3. 2. 1. Artificial Neural Network (ANN)

Artificial neural network (ANN) is a powerful technique to model the data with complicated interaction between the input/output parameters. The unique characteristics of neural networks caused to the evolution of this approach as a good alternative to determine the nonlinear dependency and extensively used in the processing of materials, e.g. simulation of the behavior of complex materials [32]. As shown in Figure 5, an ANN structure is generally separated into three sections: the input layer, the hidden layer, and the output layer. The nodes or neurons are connected by weights, which is similar to the intensity of the bioelectric transfer between node cells in a real neural network. Trained results can be summarized in terms of weight and bias [33]. The number of neurons in the output and input layers are equal to the output and input parameters, while the hidden layer is more than one layer and the number of neurons in each layer is tolerated. Network structure adjustment plays a key role in improving network performance [34].

$$N_{in} - [N_1 - N_2 - \dots - N_h]h - N_{out} \tag{6}$$

where, N_{out} and N_{in} refer to the number of output and input variables, respectively. Subscript h shows the number of hidden layers, and N_h , N_1 , N_2 and are the number of neurons in any hidden layer.

The network receives data from the input layer, decomposes data into hidden layers, and next outputs through the output layer. In each output layer and hidden layer, neurons consider the output of the neurons in the previous layer as their new input. Data using the weight bias and transfer subordinate in the neuron to obtain the output as shown in Equation (7).

$$X_i^{(n)} = f \left[\sum W_{ij}^{(n)} X_i^{(n-1)} + b_j^{(n)} \right] \tag{7}$$

where, X_j^n is the output of a node j in the n^{th} layer, W_{ji}^n the weight from the node, i in $(n-1)$ the layer to node j in the n^{th} layer, and $b_j(n)$ the bias of a node j in the n^{th} layer [35].

During the training phase, the network will set up hundreds of data cycles with data, weight, and bias until it reaches the correct error level or is maximized [36]. The simulation of weight and bias can be obtained as Equation (8):

$$W_{ij}^{(n)}(k) = W_{ij}^{(n)}(k-1) - \alpha \frac{\partial E}{\partial b_j^{(n)}} \tag{8}$$

In Equation (8), α illustrates the learning rate, and k refers to the repetition [37]. Figure 6 represents the schematic representation of the connection between the output and input resultant of a neuron.

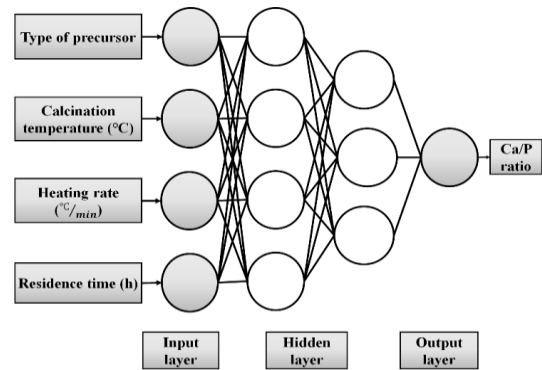


Figure 5. The schematic structure of an artificial neural network with input, output, and testing parameters

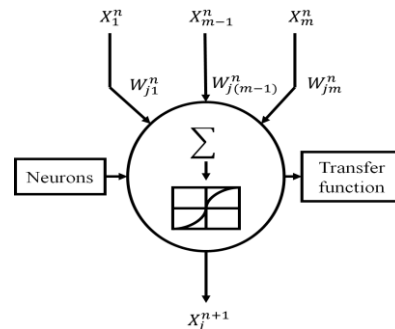


Figure 6. Schematic explanation of the connection between the output and input resultant of a neuron

3.2.2. Implementation

In general, sufficient practical data is required to create an efficient neural network. Architecture, training strategy, transfer commutable, and other elements of the neural network must attentively determine and refined to be optimized. Therefore, a well-trained neural network can be used to analyze the new input data.

An ANN performance assessment coming back to step 2 if the implementation is not satisfactory, uses the trained network to simulate or predict the process parameters in operational database area. In summary, ANN including the collection and application of practical information, network training and configuration, an ANN performance assessment, coming back to step 2 in the case that the implementation is not satisfactory and use of trained network to simulate or predict the process parameters.

3.2.3. Evaluation of the Existing Models

In present study, 70 experiments were utilized for training, and 30 for testing of ANN models through the prediction of Ca/P ratio. The inputs and output are the same as GEP modeling.

3.2.4. ANN Model Results

Figure 7 represents the linear regression plots of appropriate model through training of neural network.

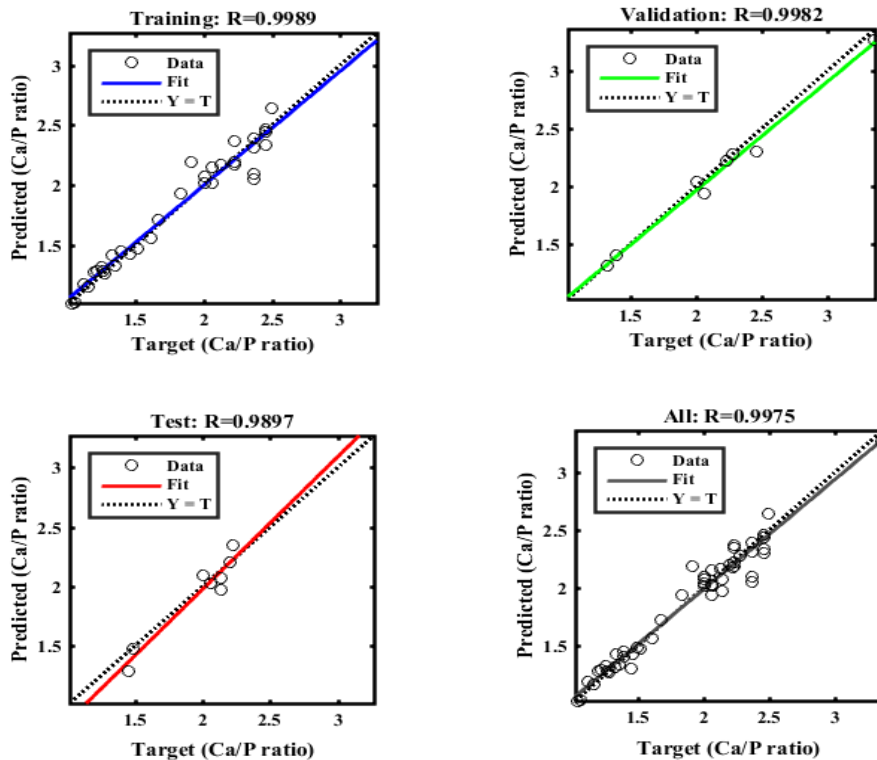


Figure 7. Regression plots of the trained neural network model that shows the linear regression factor for training, testing, validation, and all the data set

4. RESULTS AND DISCUSSION

Based on the experimental data and EDX analysis, it is found that by decreasing Ca/P ratio, the crystalline index is increased in the BC sample. Comparison of empirical and predicted values by GEP and ANN models for the Ca/P ratio are shown in Figures 4 and 7, respectively. Accordingly, the best constructed model by GEP has $MSE = 0.0015$ and $R^2 = 0.9784$ in testing and $MSE = 0.008$ and $R^2 = 0.9863$ in training. While, the best ANN model has $MSE = 1.81$ and $R^2 = 0.9897$ in testing and $MSE = 0.9800$ and $R^2 = 0.9989$ in training. Since the error indices in both models are less than 3% [24], R^2 was used as a criterion and model ANN was selected for further analysis.

4.1. Sensitivity Analysis of the ANN Model

To determine the effective parameters in the pyrolysis condition on the Ca/P ratio, sensitivity analysis has been used by employment of ANN model. In this analysis, a step-by-step approach to ANN is performed by changing each of the input parameters once at a constant speed. In this study, various constants are obtained at 2, 6, and 10%. For each input parameter, the output percentage is changed due to the variation in the input parameter. The sensitivity of each input parameter is calculated using Equation (9).

$$S_i(\%) = \frac{1}{N} \sum_{j=1}^N \left(\frac{\% \text{ Change in output}}{\% \text{ Change in input}} \right)_j \times 100 \quad (9)$$

where, S_i (%) represented the sensitivity of an input parameter, and N is refers to the number of data set used to test the network. Figure 8 shows the results of sensitivity analysis. It shows that residence time is the most effective parameters in the Ca/P ratio, while precursor type has a relatively smaller effect on it. Furthermore, it shows that any increase in residence time increases the Ca/P ratio and decrease the crystalline index. The results of GEP and ANN are relatively similar to the empirical results, and confirm the conclusive role of residence time and type of precursor on Ca/P ratio. Since the reaction happens through calcination, the effect of residence time is considered along with the type of precursor on the values of the Ca/P ratio, which is shown in the 3D surface plot in Figure 9 (a). This surface is plotted for calcination temperature of 700 °C, and 10 °C/min heating rate. To better understand the 3D surface, the contourplot is depicted in Figure 9 (b). The shaded region shows the extrapolation area of the model, which can be used for other conditions of pyrolysis. This, along with the unshaded region confirmed the above explanation.

4. 2. Confirmation Test To ensure the accuracy of the proposed model by ANN, a confirmation test is done. In this regard, the BC sample is prepared using un-activated crushed bone at the temperature of 700 °C, 10°C/min heating rate and 2 h residence time. As shown in Table 4, the predicted value of Ca/P ratio in the ANN model is 2.52, while based on EDX analysis the actual value of this ratio is 2.55. This consistency indicates the high accuracy of GEP model. Figure 10 shows the EDX spectrum of this sample.

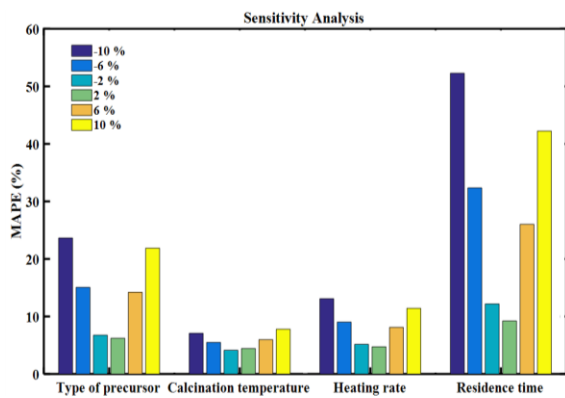


Figure 8. Comparison of the effect of the type of precursor, calcination temperature, heating rate, residence time on Ca/P ratio using sensitivity analysis

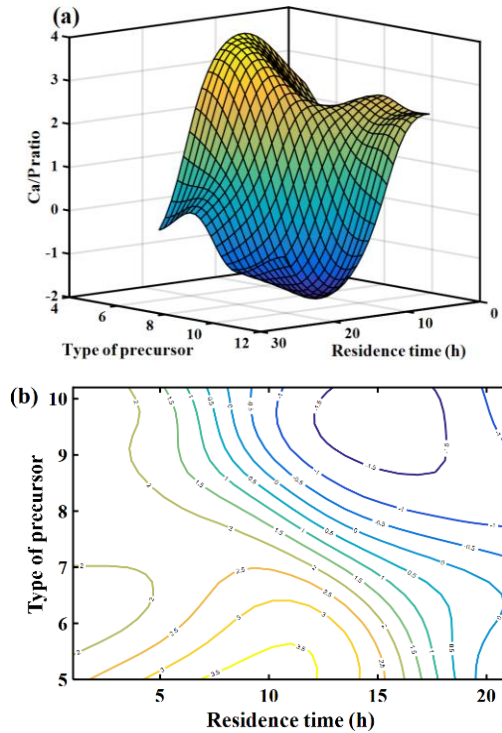


Figure 9. (a) 3D surface plot of Ca/P ratio that predicts by ANN model in calcination temperature of 700°C and heating rate 10°C/min; (b) the contour plot of the 3D surface; the shaded area shows the extrapolation region of ANN model.

TABLE 4. EDX spectrum of the validation test (un-activated crushed bone that heated at 10°C/min heating rate to 700°C, and residence time 2 h)

O	48.96
Na	0.92
Mg	0.42
P	13.78
S	0.74
Ca	35.17

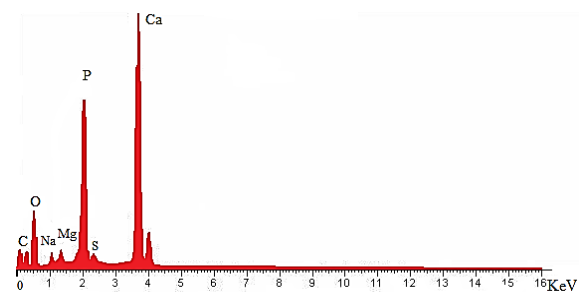


Figure 10. EDX Spectrum of prepared BC using un-activated crushed bone that heated at heating rate 10°C/min to 700°C, and residence time 2 h

5. CONCLUSION

In this study, various pyrolysis conditions used to produce BC. ANN and GEP techniques are employed to model the Ca/P ratio based on the practical conditions. In summary:

- 1: BC is prepared from crushed bone as precursor in the form of as-cleaned and activated by HNO₃ in pyrolysis technique;
- 2: Data collection is done using the design of experiment by consideration of heating rate, the type of precursor, calcination temperature, and residence time as practical parameters;
- 3: The Ca/P ratio selects as criteria for the estimation of the crystalline index of BC;
4. The excellent ability of ANN and GEP techniques are proved to model the Ca/P ratio based on pyrolysis conditions;
5. By consideration of R squared, ANN has the higher accuracy with respect to GEP to model the Ca/P ratio;
6. Validation of results is done using confirmation test;
7. Sensitivity analysis of proposed ANN model revealed that the residence time and the type of precursor in regular are the most effective parameters on Ca/P ratio.

7. REFERENCES

1. Alkurdi, S.S., Al-Juboori, R.A., Bundschuh, J., Bowtell, L. and McKnight, S., "Effect of pyrolysis conditions on bone char characterization and its ability for arsenic and fluoride removal", *Environmental Pollution*, Vol. 262, (2020), 114221. <https://doi.org/10.1016/j.envpol.2020.114221>
2. Leinweber, P., Hagemann, P., Kebelmann, L., Kebelmann, K. and Morshedizad, M., Bone char as a novel phosphorus fertilizer, In Phosphorus recovery and recycling. 2019, Springer. 419-432. https://doi.org/10.1007/978-981-10-8031-9_29
3. Dotto, G.L., Salau, N.P.G., Piccin, J.S., Cadaval, T.R.S.A. and de Pinto, L.A.A., Adsorption kinetics in liquid phase: Modeling for discontinuous and continuous systems, In Adsorption processes for water treatment and purification. 2017, Springer. 53-76.
4. de Melo, N.H., de Oliveira Ferreira, M.E., Neto, E.M.S., Martins, P.R. and Ostroski, I.C., "Evaluation of the adsorption process using activated bone char functionalized with magnetite nanoparticles", *Environmental Nanotechnology, Monitoring & Management*, Vol. 10, (2018), 427-434. <https://doi.org/10.1016/j.enmm.2018.10.005>
5. Wang, M., Liu, Y., Yao, Y., Han, L. and Liu, X., "Comparative evaluation of bone chars derived from bovine parts: Physicochemical properties and copper sorption behavior", *Science of The Total Environment*, Vol. 700, (2020), 134470. <https://doi.org/10.1016/j.scitotenv.2019.134470>
6. Dalvand, H., Khayati, G.R., Darezereshki, E. and Irannejad, A., "A facile fabrication of nio nanoparticles from spent ni-cd batteries", *Materials Letters*, Vol. 130, (2014), 54-56. <https://doi.org/10.1016/j.matlet.2014.05.057>
7. Medellin-Castillo, N.A., Padilla-Ortega, E., Tovar-García, L.D., Leyva-Ramos, R., Ocampo-Pérez, R., Carrasco-Marín, F. and Berber-Mendoza, M.S.J.A., "Removal of fluoride from aqueous solution using acid and thermally treated bone char", *Adsorption*, Vol. 22, No. 7, (2016), 951-961. <https://doi.org/10.1007/s10450-016-9802-0>
8. Zhao, J., Zhao, J., Chen, J., Wang, X., Han, Z. and Li, Y., "Rietveld refinement of hydroxyapatite, tricalcium phosphate and biphasic materials prepared by solution combustion method", *Ceramics International*, Vol. 40, No. 2, (2014), 3379-3388. <https://doi.org/10.1016/j.ceramint.2013.09.094>
9. Levinskas, G.J. and Neuman, W.F., "The solubility of bone mineral. I. Solubility studies of synthetic hydroxylapatite", *The Journal of Physical Chemistry*, Vol. 59, No. 2, (1955), 164-168. <https://doi.org/10.1021/j150524a017>
10. Cheung, C.W., Chan, C.K., Porter, J.F. and McKay, G., "Combined diffusion model for the sorption of cadmium, copper, and zinc ions onto bone char", *Environmental Science & Technology*, Vol. 35, No. 7, (2001), 1511-1522. <https://doi.org/10.1021/es0012725>
11. Medellin-Castillo, N.A., Leyva-Ramos, R., Ocampo-Perez, R., Garcia de la Cruz, R.F., Aragon-Pina, A., Martinez-Rosales, J.M., Guerrero-Coronado, R.M. and Fuentes-Rubio, L., "Adsorption of fluoride from water solution on bone char", *Industrial & Engineering Chemistry Research*, Vol. 46, No. 26, (2007), 9205-9212. <https://doi.org/10.1021/ie070023n>
12. Warren, G., Robinson, J. and Someus, E., "Dissolution of phosphorus from animal bone char in 12 soils", *Nutrient Cycling in Agroecosystems*, Vol. 84, No. 2, (2009), 167-178. <https://doi.org/10.1007/s10705-008-9235-6>
13. Siebers, N. and Leinweber, P., "Bone char: A clean and renewable phosphorus fertilizer with cadmium immobilization capability", *Journal of Environmental Quality*, Vol. 42, No. 2, (2013), 405-411. <https://doi.org/10.2134/jeq2012.0363>
14. Medellin-Castillo, N., Leyva-Ramos, R., Padilla-Ortega, E., Perez, R.O., Flores-Cano, J. and Berber-Mendoza, M., "Adsorption capacity of bone char for removing fluoride from water solution. Role of hydroxyapatite content, adsorption mechanism and competing anions", *Journal of Industrial and Engineering Chemistry*, Vol. 20, No. 6, (2014), 4014-4021. <https://doi.org/10.1016/j.jiec.2013.12.105>
15. Rojas-Mayorga, C.K., Silvestre-Alberio, J., Aguayo-Villarreal, I.A., Mendoza-Castillo, D.I. and Bonilla-Petriciolet, A., "A new synthesis route for bone chars using co₂ atmosphere and their application as fluoride adsorbents", *Microporous and Mesoporous Materials*, Vol. 209, (2015), 38-44. <https://doi.org/10.1016/j.micromeso.2014.09.002>
16. Zwetsloot, M.J., Lehmann, J. and Solomon, D., "Recycling slaughterhouse waste into fertilizer: How do pyrolysis temperature and biomass additions affect phosphorus availability and chemistry?", *Journal of the Science of Food and Agriculture*, Vol. 95, No. 2, (2015), 281-288. <https://doi.org/10.1002/jsfa.6716>
17. Zwetsloot, M.J., Lehmann, J., Bauerle, T., Vanek, S., Hestrin, R. and Nigussie, A., "Phosphorus availability from bone char in a p-fixing soil influenced by root-mycorrhizae-biochar interactions", *Plant and Soil*, Vol. 408, No. 1-2, (2016), 95-105. <https://doi.org/10.1007/s11104-016-2905-2>
18. Morshedizad, M., Zimmer, D. and Leinweber, P., "Effect of bone chars on phosphorus-cadmium-interactions as evaluated by three extraction procedures", *Journal of Plant Nutrition and Soil Science*, Vol. 179, No. 3, (2016), 388-398. <https://doi.org/10.1002/jpln.201500604>
19. Flores-Cano, J.V., Leyva-Ramos, R., Carrasco-Marín, F., Aragón-Piña, A., Salazar-Rabago, J.J. and Leyva-Ramos, S., "Adsorption mechanism of chromium (iii) from water solution on bone char: Effect of operating conditions", *Adsorption*, Vol. 22, No. 3, (2016), 297-308. <https://doi.org/10.1007/s10450-016-9771-3>

20. Iriarte-Velasco, U., Sierra, I., Zudaire, L. and Ayastuy, J.L., "Preparation of a porous biochar from the acid activation of pork bones", *Food and Bioproducts Processing*, Vol. 98, No., (2016), 341-353. <https://doi.org/10.1016/j.fbp.2016.03.003>
21. Robinson, J.S., Baumann, K., Hu, Y., Hagemann, P., Keblmann, L. and Leinweber, P., "Phosphorus transformations in plant-based and bio-waste materials induced by pyrolysis", *Ambio*, Vol. 47, No. 1, (2018), 73-82. <https://doi.org/10.1007/s13280-017-0990-y>
22. Jia, P., Tan, H., Liu, K. and Gao, W., "Synthesis and photocatalytic performance of zno/bone char composite", *Materials*, Vol. 11, No. 10, (2018), 1981. <https://doi.org/10.3390/ma11101981>
23. Koza, J.R. and Koza, J.R., "Genetic programming: on the programming of computers by means of natural selection" (Vol. 1), MIT press, 1992.
24. de Castilho, V.C., El Debs, M.K. and do Carmo Nicoletti, M., "Using a modified genetic algorithm to minimize the production costs for slabs of precast prestressed concrete joists", *Engineering Applications of Artificial Intelligence*, Vol. 20, No. 4, (2007), 519-530. <https://doi.org/10.1016/j.engappai.2006.09.003>
25. Ferreira, C., "Gene expression programming: A new adaptive algorithm for solving problems", *Complex Systems*, Vol. 13, No. 2, (2001), 87-129. [arXiv:cs/0102027](https://arxiv.org/abs/cs/0102027)
26. Cheng, M.-Y., Firdausi, P.M. and Prayogo, D.J.E.A.o.A.I., "High-performance concrete compressive strength prediction using genetic weighted pyramid operation tree (gwpot)", *Engineering Applications of Artificial Intelligence*, Vol. 29, No., (2014), 104-113. <https://doi.org/10.1016/j.engappai.2013.11.014>
27. Ferreira, C., "Gene expression programming: Mathematical modeling by an artificial intelligence, Springer, Vol. 21, (2006).
28. Ong, C.S., Huang, J.J. and Tzeng, G.H., "Building credit scoring models using genetic programming". *Expert Systems with Applications*, Vol. 29, No. 1, (2005), 41-47. <https://doi.org/10.1016/j.eswa.2005.01.003>
29. Mollahasani, A., Alavi, A.H., Gandomi, A.H.J.C. and Geotechnics, "Empirical modeling of plate load test moduli of soil via gene expression programming", Vol. 38, No. 2, (2011), 281-286. <https://doi.org/10.1016/j.compgeo.2010.11.008>
30. Hosseini, M., Khayati, G.R., Mahdavi, M. and Danesh-Manesh, H., "Modeling and optimization of roll-bonding parameters for bond strength of ti/cu/ti clad composites by artificial neural networks and genetic algorithm", *International Journal of Engineering, Transactions C: Aspects*, Vol. 30, No. 12, (2017), 1885-1893. <https://doi.org/10.5829/ije.2017.30.12c.10>
31. Si, H.Z., Wang, T., Zhang, K.J., De Hu, Z., Fan, B.T.J.B. and Chemistry, M., "Qsar study of 1, 4-dihydropyridine calcium channel antagonists based on gene expression programming", *Bioorganic & Medicinal Chemistry*, Vol. 14, No. 14, (2006), 4834-4841. <https://doi.org/10.1016/j.bmc.2006.03.019>
32. Guessasma, S., Montavon, G. and Coddet, C., "Neural computation to predict in-flight particle characteristic dependences from processing parameters in the aps process", *Journal of Thermal Spray Technology*, Vol. 13, No. 4, (2004), 570-585. <https://doi.org/10.1361/10599630419391>
33. Austin, N., Kumar, P.S. and Kanthavelkumaran, N., "Artificial neural network involved in the action of optimum mixed refrigerant (domestic refrigerator)", *International Journal of Engineering-Transactions A: Basics*, Vol., No., (2013), 1235-1242. <https://doi.org/10.5829/idosi.ije.2013.26.10a.13>
34. Pradeep, J., Srinivasan, E. and Himavathi, S., "Neural network based recognition system integrating feature extraction and classification for english handwriting", *International Journal of Engineering, Transactions B: Applications*, Vol. 25, No. 2, (2012), 99-106. <https://doi.org/10.5829/idosi.ije.2012.25.02b.03>
35. Khanmohammadi, S., "Neural network modelling of optimal robot movement using branch and bound tree", *International Journal of Engineering*, Vol. 7, No. 2, (1994), 95-110. Retrieved from: http://www.ije.ir/article_71101_2db276aad3a417e1836645f7e4b24984.pdf
36. Mahdavi, M. and Khayati, G.R., "Artificial neural network based prediction hardness of al2024-multiwall carbon nanotube composite prepared by mechanical alloying", *International Journal of Engineering, Transactions C: Aspects*, Vol. 29, No. 12, (2016), 1726-1733. <https://doi.org/10.5829/idosi.ije.2016.29.12c.11>
37. Neshat, E. and Saray, R.K., "An optimized chemical kinetic mechanism for hcci combustion of prfs using multi-zone model and genetic algorithm", *Energy Conversion and Management*, Vol. 92, No., (2015), 172-183. <https://doi.org/10.1016/j.enconman.2014.11.057>

Persian Abstract

چکیده

زغال استخوان یکی از رایج‌ترین انواع جاذب با کاربردهای گسترده برای از بین بردن آلودگی‌ها می‌باشد. توانایی جذب این ماده به شاخص کریستالی آن وابسته است، که از طریق نسبت Ca/P معین می‌شود. در این تحقیق تلاش شد که شاخص کریستالی زغال استخوان از طریق مدل‌سازی شرایط تجزیه‌ی حرارتی این ماده توسط شبکه‌ی عصبی مصنوعی و برنامه‌ریزی بیان ژنتیکی انجام شود. به همین منظور ۱۰۰ داده‌ی تجربی متفاوت به صورت جداگانه برای ساخت مدل‌های شبکه‌ی عصبی مصنوعی و برنامه‌نویسی بیان ژنتیک مورد استفاده قرار گرفت. در مرحله‌ی جمع‌آوری داده‌های تجربی، آهنگ گرمایش، نوع فعال‌ساز، دمای کلیسیناسیون و مدت زمان نگهداری نمونه‌ها به عنوان داده‌های ورودی، و نسبت Ca/P به عنوان خروجی تعیین شد. نتایج نشان داد که با آهنگ گرمایش ۱۰ درجه‌ی سانتی‌گراد بردقیقه، دمای کلیسیناسیون ۱۰۰۰ درجه‌ی سانتی‌گراد و مدت زمان نگهداری ۲ ساعت باعث دست‌یابی به کمترین میزان نسبت Ca/P خواهد شد. از شاخص ضریب تعیین برای مقایسه‌ی عملکرد مدل‌های استخراج شده از شبکه‌ی عصبی مصنوعی و برنامه‌نویسی بیان ژنتیکی استفاده شد. در نهایت، بهترین مدل شبکه‌ی عصبی مصنوعی برای تحقیق در مورد تاثیر هر یک از متغیرهای عملی بر روی شاخص کریستالی از طریق آنالیز حساسیت استفاده شد. مشخص شد که زمان نگهداری نمونه موثرترین پارامتر در تعیین شاخص کریستالی ماده است، در حالی که نوع فعال‌ساز اهمیت کمتری دارد.
